CHEMICAL PROBLEMS OF THE DEVELOPMENT OF NEW MATERIALS AND TECHNOLOGIES
Minsk 2003

D. V. Sviridov

ION IMPLANTATION IN POLYMERS: CHEMICAL ASPECTS

INTRODUCTION

Ion implantation technique, initially developed for microelectronic applications, has also shown itself as a powerful tool for the surface engineering in case of polymeric materials. The ion-beam treatment results in the fundamental changes in the electrical, optical, rheological and sorption properties of polymers as well as their microhardness, wear resistance and biocompatibility. Of special interest is the fact of drastic increase (by 10–15 orders of magnitude) of conductivity of normally insulating polymers as the result of ion irradiation that opens up possibilities for novel polymer-based electronic devices.

This chapter generalizes results of the studies on the ion beam-modified polymers which has been performed in the last years in Byelorussian State University by joined forces of chemists and physicians. In these investigations the emphasis was given on the elucidation of the exact structure of the implanted layer and ion beam-produced nanostructurated carbonaceous phase responsible for the conductivity of the ion-irradiated polymers.

ION INTERACTION WITH POLYMER TARGET: BASIC PRINCIPLES

The characteristic property of ion implantation is the high density of the energy deposited in the irradiated sample: the energy losses of an incoming ion in the polymer target range up to tens and hundreds of electron-volts per Å, this energy being released in a small volume along the ion track within a very short time period (~10^{-14} seconds). Taking into account the fact that the bond dissociation energies in polymers do not exceed 10 eV (*e.g.*, 4.3 eV for the C–H and 9.3 eV for the C=N bond), the energy transferred from the stopping projectile appears to be high enough to break a large number of chemical bonds even in the case of implantation of medium-range energy (from tens to hundreds of keVs) ions. This, in its turn, creates prerequisites for deep transformations in the irradiated polymer during ion bombardment [1–3].

The energy released by the particle during slowing down is deposited to the target by means of two basically different mechanisms, (i) electronic excitation and (ii) nuclear collision, which are able to induce quite different processes of polymer matrix rearrangement. The former mechanism leads to excitation and ionization of polymer molecules and, as a result, to the formation (both directly and

due to fast sequent neutralization) of a large number of mobile radical species (first of all, $H^{\cdot}$ radicals) and polymer macroradicals. Nuclear collisions are accompanied by massive breakage of chemical bonds due to displacements of atomic nuclei and by transfer of rather high energy to the polymer matrix in the form of phonons. After transfer of sufficiently high energy, the displaced atoms can, in turn, create their own track cascades (Fig. 1). Both mechanisms act simultaneously and their additive contribution to the total energy losses of the incoming ion is characterized by stopping power (S_e for the electronic mechanism and S_n for the nuclear one, respectively) which represents the change in the energy of ion caused by its interaction with the polymer matrix per path length and is usually expressed in eV/Å. The values of S_e and S_n depend on the energy and mass of the implanted ion as well as on the polymer composition, the energetic light ions depositing the energy mainly *via* electronic excitations while the energy transfer from low-energy heavy ions occurring predominantly through nuclear collisions. As the ion slows down, the contribution of each mechanism to the overall energy loss substantially changes (*e.g.*, a feature of light ions is an increase in the relative weight of «nuclear» energy loss at the end of the ion track – for illustration see Fig. 1).

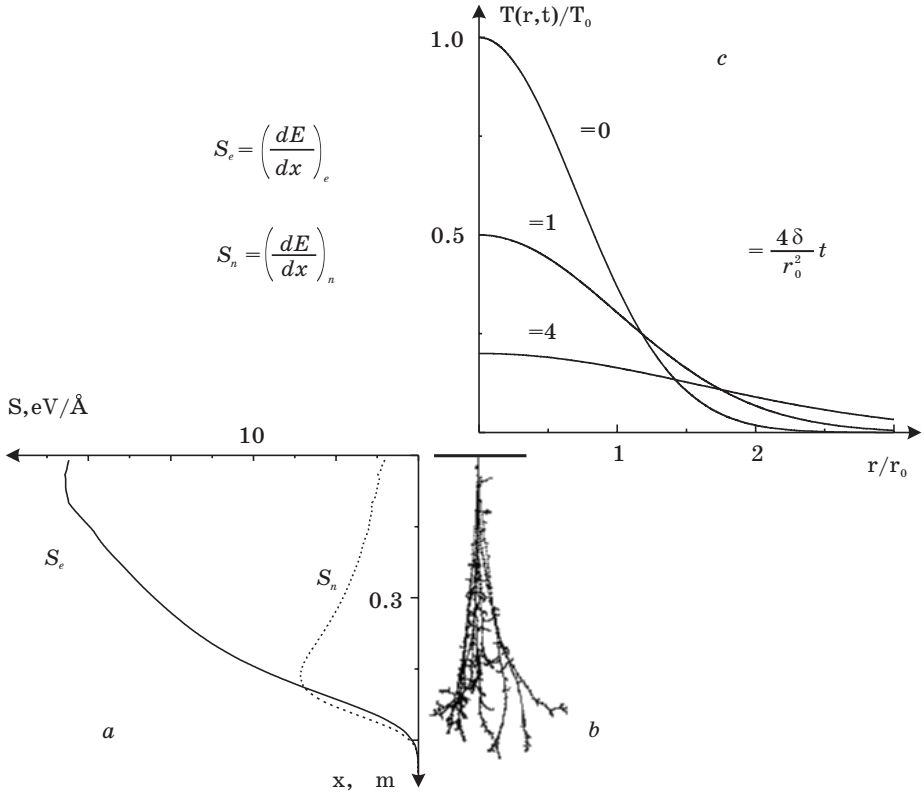

Fig. 1. (*a*) Energy loss parameters versus penetration depth and (*b*) trajectories of 100-keV B^+ implanted into polyethylene (the Monte-Carlo simulations with the use of TRIM code); (*c*) temperature distribution in the ion track region and its evolution with time (in the dimensionless variables)

The stopping of the incoming ions in the polymer matrix is accompanied by deposition of high energy interior the track and leads to the formation of radicals, secondary ions and electrons. Certain parts of the electrons possesses enough energy to leave the track of the passed ion and their own secondary tracks form a region of so-called penumbra. The radius of the «core» of the ion track depends on the energy of the projectile and on the energy deposition mechanism. For ions with energies of several hundreds of keV to one MeV per nucleon, the estimate for the core radius gives ~ 5–10 Å, while the penumbra's radius is about 50–100 Å. The average density of energy released beyond the track core is far less than inside and the chemical processes occurring within the penumbra can be thus considered pure radiation ones. By contrast, the track core turns out to be heated up to very high temperatures. The dependence of the local temperature, $T(r, t)$, in the cylindrical track region on the radial distance from the particle trajectory, r, and on the time elapsed since the passage of the implanted ion, t, can be described in the framework of the well-known «thermal spike» model in the following manner:

$$T(r, t) \quad \frac{T_0}{1 \quad 4\delta /r_0^2} \exp \quad \frac{(r / r_0)^2}{1 \quad 4\delta /r_0^2}, \qquad T_0 \quad \frac{\gamma S}{\pi D C_v r_0^2}, \tag{1}$$

where r_0 is a track core radius, δ is the thermal diffusivity of the medium, T_0 is the initial temperature, D is the polymer density, C_v is the heat capacity, S is the overall stopping power, and γ is the portion of the deposited energy converted to heat in the track core. The time-dependent temperature profile calculated *via* Eq. (1) is shown in Fig. 1. It is seen from the figure that when the temperature in the track decreases, only a slight widening of the heating zone is observed. For 0,1–1 MeV ions implanted in different polymers (polyethylene, polyimide, polyamide), the calculated initial temperatures are on the order of 10^4 K, and the time between reaching the peak temperature and decaying to the original level corresponding to the temperature of the polymer target under ion irradiation (*ca.* 100–150 °C) is about 10^{-9} s. This model gives only a rough estimation of T_o and the characteristic time of thermal pulse, but does quite well in predicting the order of the excess temperature and the time scale over which the temperature jump occurs.

It should be noted that the chemical reactions occurring in the polymer matrix during the ion implantation cannot be considered neither in terms of thermolysis (despite high peak temperatures in the track) nor in terms of radiolysis and represent an unified process of radiothermolysis [1–3]. Thermal and radiative components of this process interplay in a complex manner because the radicals produced *via* radiolysis and the products of their relaxation are involved in the pyrolytic conversion processes. Moreover, since the ion-induced reactions of polymer transformation turn out to be confined in a small volume, there is a threshold fluence, Φ_f, at which the sample surface appears to be completely «filled» with ion tracks and further implantation is thus performed into already modified material. Therefore, taking into consideration this geometric factor, it is reasonable to recognize at least two fluence regimes: a single track regime in which the each track in the polymer host is isolated from the others and a track overlapping regime, these two implantation regimes corresponding to different steps of the ion-induced polymer modification.

ION BEAM-INDUCED CHEMICAL PROCESSES IN THE POLYMER MATRIX

In the case of carbon-containing polymers the main consequence of high-dose implantation is the carbonization of the irradiated surface [1–4]. This process is accompanied by the emission of large amounts of gaseous compounds (H_2, low-molecular hydrocarbons as well as CO and CO_2 in case of oxygen-containing polymers) and eventually results in the formation of a dense carbon-rich surface layer that generally shows Raman spectra analogous to those of amorphous hydrogenated carbons. The exact mechanism of carbonaceous phase formation, however, still remains unclear in many aspects because of apparent experimental difficulties (the complex nature of ion-polymer interactions results in very complex chemical response). Therefore we shall restrict our consideration to the most general pattern of the ion beam-induced radio- and thermochemical processes occurring in the polymer host during ion bombardment.

It has been noted above that the thermally-induced processes occurring during the implantation are coupled with radiation-induced ones that involve the excited polymer units, cation-radicals and trapped electrons. In the case of polyethylene (which is the simplest one of polyolefines), the relaxation of the excited polymer units results in formation of alkyl macroradicals and $H^{\cdot}$ radicals. This radicals can recombine or interact with the polymer yielding molecular hydrogen and double bonds in the polymer chains. Ionized polymer units predominantly recombine within the track volume with the trapped electrons, leading to excited polymer units, or are converted into either alkyl radicals or olefinic cation-radicals *via* deprotonation and H_2 elimination, respectively. These radiation-induced processes, which occur both in the track core and the penumbra, appear to be responsible to a substantial extend for the emission of hydrogen, which is the major gaseous product formed in course of ion implantation (in contrast to the conventional vacuum pyrolysis of polyethylene, which leads to an assortment of hydrocarbons). The radicals and unsaturated products formed are involved in pyrolysis reactions within the thermal spike or accumulate in the implanted layer to be expended at subsequent steps of the implantation.

The processes discussed above also result in cross-linking of macromolecules. Thus, for polyethylene the ratio of radiation yields of cross-linking and scission is known to be between 3 and 5 and ion implantation results in the polymer cross-linking, this process being concentrated mostly between lamellae because of the high mobility of free valences. Since the radius of penumbra is much greater than the track core radius, the polymer cross-linking turns out to be completed at fluences that are 1.5–2 orders of magnitude lower than Φ_f and further implantation is thus performed into a cross-linked polymer.

In general, the following thermochemical processes occur within the thermal spike [1–4]: (i) destruction of the polymer molecules, (ii) cyclization and aromatization, and (iii) condensation of the cyclic compounds. The process of the first type proceeds effectively at temperatures above 250–400 ^{o}C and in the case of polyethylene results in polymer backbone fragmentation. At the temperatures higher than 800 ^{o}C aromatic hydrocarbons become more stable than linear saturated and unsaturated ones and in the closed system cyclization with the formation of aromatics

occurs. The cyclization, which appears to occur through intramolecular diene synthesis (Diels-Alder-type mechanism), is favored by the formation of conjugated compounds and macroradicals as well as by the polymer chain fragmentation at a previous stage of the polymer radiopyrolytic conversion in the track, the role of the allyle and polyenyle radical in formation of cyclic products being dependent on the dehydrogenation degree achieved to the moment when the temperature in the track falls below ~ 800 °C. At lower temperatures (400–500 °C) the aromatic compounds formed are involved in the reaction of condensation, being additionally stabilized by an increase of the resonance energy. Processes (ii) and (iii) are accompanied by hydrogen elimination and, alongside with radiolysis processes, contribute into the H_2 emission. Along with hydrogen, the emission of hydrocarbons of different molecular weights also occurs during ion implantation, the highest emission yield being observed for acetylene which is known to be the most stable acyclic hydrocarbon at high temperatures. Some hydrocarbon molecules produced in the track obviously have a chance to undergo pyrolytic conversion, but the role of this process in the carbonaceous phase formation still remains unclear.

Planar multiple ring structures (primitive π-bonded carbon clusters), unsaturated compounds, and macroradicals produced in the single-track regime are the precursors of the carbon clusters (*i.e.*, the fragments of graphite sheets) that are formed in the course of a successive overlapping of the ion tracks in the irradiated area during further ion bombardment [1–4].

Depending on the mechanism of energy transfer from incident ions to the polymer matrix, essentially different chemical reactions are induced. In particular, nuclear collisions lead to direct bond breaking, whereas the energy deposition by means of the electronic stopping mechanism results in excitation of the polymer units. Taking into account that the excitation within the lifetime (*ca.* 10^{-12} s) can migrate to a large distance (the mean path range for excitation migrating along the aliphatic chain was estimated theoretically to reach a length of 100 polymer units), one could conclude that the electronic deposition mechanism furnishes the scission of the most weak bonds. The difference between the electronic and collisional energy deposition mechanisms is most conspicuous in the case of the polymers with heteroatom-containing functional groups. It is evident that binary collisions will result in random bond rupture, while the electronic mechanism provides selective scission of definite bonds in the course of relaxation of the excited state, and the mobile $H^{\bullet}$ radicals massively produced in the track also react with the polymer host in a selective manner. For example, when polyimide is implanted with ions having rather low S_n/S_e ratio, the selective degradation of the ether linkage and gradual conversion of the imide groups into amide ones occur.

The energy deposited in the polymer host by means of the electronic excitation is spent in the reactions of dehydrogenation and weak bond breaking but without rupture of the aromatic fragments, which can be involved in condensation processes yielding the polyaromatic structures. Within a certain 'incubation' fluence, which is generally consistent with Φ_f, the total concentration of heteroatoms in the implanted layer (*e.g.*, nitrogen content in the implanted polyimide) can remain almost constant, whereas the progressive loss of heteroatoms being observed at further stages of the polymer structure rearrangement in the course of ion bombardment. This rearrangement is consistent with the growth of the initial carbon

clusters, which presumably occurs through condensation of the ion-induced aromatic, polyaromatic and unsaturated fragments, the heteroatoms being involved in this process forming pyridine-like, pyran and thiopyran cycles. The incorporation of heteroatoms in the carbon network seems to be responsible for the fact that considerable amounts of sulphur and nitrogen remain in the implanted layer even at very high fluencies.

The carbonization of the polymer surface under the bombardment is generally completed at fluenes of $10^{16} - 5 \times 10^{16}$ cm^{-2}, with further implantation being accompanied by only minor changes in the composition and structure of the implanted layer. Thus, for instance, the Rutherford Back Scattering (RBS) measurements evidence that during the ion implantation of polyethylene with 150-keV F^+ ions ($S_n/S_e \approx 0.2$), the carbon content in the implanted layer saturates at 40 % (the carbon content in pristine polyethylene is 33 %). In this range of energies the degree of the polymer dehydrogenation rises as the collisional mechanism of energy deposition becomes predominant; thus the carbon concentration at the surface of polyethylene implanted with 150-keV As^+ ions ($S_n/S_e \approx 3$) saturates at the level of 65 %. The lower dehydrogenation ability of projectiles that release energy to the target by means of the electronic deposition mechanism can be attributed to the effective delocalization of the excitation within the π-bonded carbon clusters and to fast cooling of the thermal spike owing to greater heat conductivity of the carbonized polymer. The bonds breaking in binary collisions provides more efficient dehydrogenation and the carbonization level attained under these conditions is governed by retrapping of hydrogen atoms by the terminated carbon bonds. A low hydrogen content (<10 %) can be also achieved within the electronic deposition mechanism when ions with energies of several tens MeV are implanted in a polymer target; in this case the hydrogenation process, due to migration of an excitation, is concentrated at the edges of growing carbon clusters and the carbonaceous phase produced by high-fluence implantation shows the Raman spectrum similar to that of the implanted graphite [1–4].

The carbon structures formed under ion implantation reinforce the polymer surface and result in a drastic increase in its hardness. Since the displacement energy of an sp^3-hybridized carbon atom in diamond is much higher than that of sp^2-hybridized atom, one can expect that nuclear collisions lead to gradual accumulation of domains with predominant sp^3-hybridized carbon atoms during the course of ion bombardment of polymer surface thus enhancing its microhardness. However, the microhardness of ion-induced carbon nanophase is first of all determined by the interconnectivity within the cluster aggregates and experimental data indicate that the maximal hardness is attained when electronic stopping dominates.

Chemical modification of the polymer during the ion implantation is also accompanied by some substantial changes in the wettability (*i.e.*, the polarity) of the irradiated surface. The variation in the polar component of the surface free energy results either from the changes in the concentration of the initial polar groups at the polymer surface and their transformation at early stages of implantation or from the oxidation of ion-implanted polymer with ambient oxygen yielding the carbonyl groups. On the other hand, the formation of surface pores additionally amplifies the wettability thus imparting the superhydrophylic properties to the ion-irradiated polymer surfaces.

THE STRUCTURE OF THE IMPLANTED LAYER

The information on the structure of the implanted layer, which is hardly to be examined with the help of transmission electron microscopy due to the parasite radiolytic action of the analyzing electron beam, comes mostly from the indirect observations, in particular from examination of the depth distribution of oxygen trapped in the irradiated polymer by employing the RBS technique.

The dangling bonds produced in the polymer host during ion bombardment react effectively with the atmospheric oxygen, and RBS studies reveal that the oxidation process extends across the whole width of the implanted layer [2, 5, 6]; according to IR spectroscopy, the oxidation of radiation-damaged polymers is accompanied by the formation of carbonyl groups [7]. High permeability of the implanted layer to oxygen (for example, the oxidation of implanted polyethylene occurs during the vacuum-open air transition) is a result of nanopores that appear along the trajectories of the implanted ions. The effective radius of these pores generally does not exceed a few Å, but their existence is beyond question being strongly supported by the possibility of effective insertion of molecules and ions into the implanted layer from a solution in contact. The investigation of the oxygen distribution in the polymer target provides significant information on the structure of the implanted layer, because the trapped oxygen decorates the regions with high concentrations of dangling bonds produced during ion bombardment. For low implantation fluences (below Φ_f), the oxygen depth profiles reconstructed from RBS spectra are generally coincident with the depth distribution of energetic losses for the incoming ion (Fig. 2). At higher fluences a significant oxygen depletion in the surface layer is observed (Fig. 2), the total amount of assimilated oxygen and the yield of carbonyl groups (*i.e.*, the number of carbonyl groups produced in the implanted layer per incident ion) diminishing with the implanted dose. This phenomenon can be attributed to the fact that in this fluence range, recombination of the terminated carbon bonds with the formation of carbon phase occurs and this process becomes dominant. Consequently, the concentration of trapped oxygen turns out to be low in the regions of the implanted layer where enrichment with carbon is most pronounced [2, 6]. At high fluences, when the implantation is performed into already carbonized polymer, the dangling carbon bonds capable of oxygen trapping are produced mostly in the collisional events, whereas the energy released to the target by the electronic mechanism is dissipated in the carbon structures and wasted in their rearrangement. Because of this, the oxygen depth profiles for polymers implanted with light ions under high-fluence regime are similar in shape to the calculated nuclear loss distributions [2, 8].

It should be noted that during the implantation of low-energy ions (*e.g.*, 100-keV B^+) in polyethylene, polyamide, and some other polymers [9–15], the carbon enrichment turns out to be maximum at some depth below the surface of the irradiated target, which is evidenced by the depth profile of carbon excess in the implanted layer reconstructed from RBS spectra [5]. In this case the oxygen depth profile is, generally, saddle-shaped because the additional maximum of oxygen concentration can appear at the surface of the irradiated sample [4,8]. The localization of the carbonization process within the polymer bulk, which results in formation of a carbon-rich layer, can be attributed to high release of heat at the end of the ion trajectory and lateral spread of the polymer radiothermolysis zone within the collision cascade volume. The possible pyrolytic conversion of low-molecu-

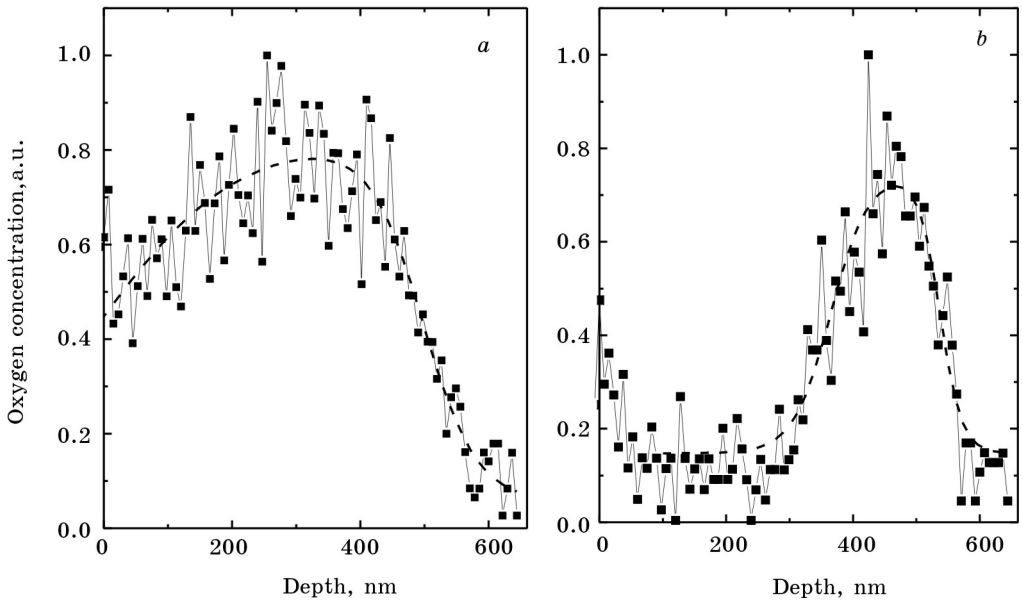

Fig. 2. Oxygen depth profiles for polyethylene implanted with (*a*) 10^{16} B^+/cm^2, (*b*) 5×10^{16} B^+/cm^2 at 100 keV. The depth profiles are reconstructed from the RBS spectra

lar hydrocarbons deep within the implanted layer could also contribute to carbonaceous phase formation, but the exact role of processes of this type remains unclear.

The porous structure and high permeability of the implanted layer facilitate the gas transport reactions in nanopores and in some cases permit the implants to escape from the irradiated polymer (both in the course of implantation and on standing); in these situations the depth distribution of the implant differs considerably from the theoretically predicted one, or there is even no signal from the implanted species in the RBS spectrum. Phenomena of this sort can be observed either when the implants do not react with the polymer host or when this reaction leads to the volatile products. Here, modest heating of the target under the ion bombardment appears to be sufficient to sublime the implanted material. Such effects are common for noble gases implanted into different polymer hosts and can also be observed for the implantation of F^+ or Sb^+ ions yielding readily evaporating products upon implantation.

A similar redistribution of the implant was observed by employing the neutron depth profiling technique in case of boron implantation into polyamide 6 and polyethylene [6] (Fig. 3). The volatile organoboranes are apt to be formed during implantation of B^+ (this is supported by the fact that atomic boron readily react with hydrocarbons). It is significant that boron alkyls at low oxygen pressure are converted into organo-oxo-boranes which are capable of being hydrolyzed into organo-hydoxy-boranes; the latter are also the volatiles that explain in the fact that the implanted boron completely leaves the polymer targets upon long-term storage.

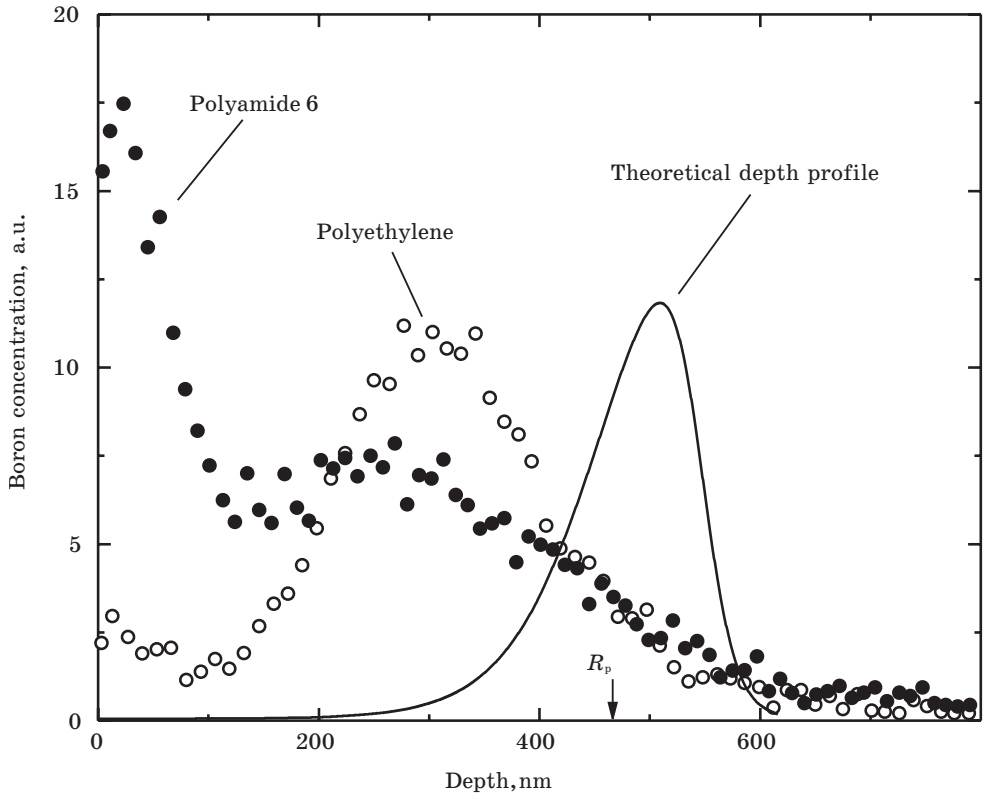

Fig. 3. Boron depth profiles for polyethylene and polyamide 6 implanted with 5×10^{16} B^+/cm^2 at 100 keV. Theoretical depth profile for boron implanted into polyethylene was calculated by TRIM code, R_p is the theoretical projected range

Notwithstanding the fact that ion implantation affects only the surface layer of the polymer target, the profound chemical modification occurring during the ion bombardment results in drastic changes in the optical characteristics of the irradiated material. In the case of transparent polymers studied (polyolefines, polyamides, polyimide), ion-induced coloration can be observed even at an implantation fluence of 10^{13} cm^{-2}, with the color changing from pale yellow to deep brown with the implanted dose; at high doses (*ca.* 10^{17} cm^{-2}) the polymer surface becomes grayish silver with a metallic luster. These color changes are accompanied by a gradual bathochromic shift of the absorption edge, a high level of light scattering being inherent in heavily dosed polymer films. The adsorption spectra of the implanted polymers are smooth, but in case of polyolefines implanted with very low doses ($10^{12} - 5 \times 10^{13}$ cm^{-2}) a weakly pronounced fine structure is observed at the wavelengths of 220–300 nm [7]; these additional maxima in the absorption spectra could be attributed to either conjugated double bonds produced in the polymer host upon implantation or carbon clusters of subnanometer size. At higher fluences the shape of the spectrum is determined by the absorption by π-bonded carbon clusters and the observed red shift of the absorption edge originating from the carbon clusters growth can be considered as a quantum-size effect of special

type. This allows us to estimate the size of the carbon clusters (or, more precisely, the size of the largest clusters) from the optical absorption data [7]. If the absorption induced by ion bombardment is due solely to π-electrons, the number of fused six-fold benzoid rings in the two-dimensional finite carbon cluster can be estimated by means of the relation, initially derived to describe the absorption of amorphous carbons:

$$E_g \quad 2|\beta|N^{\ 0.5}, \tag{2}$$

where E_g is the optical gap for a given fluence, which can be evaluated from Tauc plot, N is the number of benzoid rings that form the cluster, β is the resonance integral (according to EHT calculations, β = 2.9 eV). The fluence dependence of E_g for ion-implanted polymers can be usually fitted with an exponential function,

$$E_g \quad E_{g0} \quad A\exp(\ \varepsilon\Phi),$$

where E_{g0} is the optical gap corresponding to the completion of cluster growth, ε is the cross-section for the cluster growth process, A is a constant. For polyolefines (*e.g.*, for polyethylene) implanted with 100–300 keV light ions, the E_g value saturates at *ca.* 0.6 eV (Fig. 4), which corresponds to clusters with a mean size of *ca.* 2.7 nm (~75 benzoid rings); however, peculiar to the irradiation of polyamide 6 under the same conditions is the formation of smaller clusters (E_{g0} = 0.76 eV,

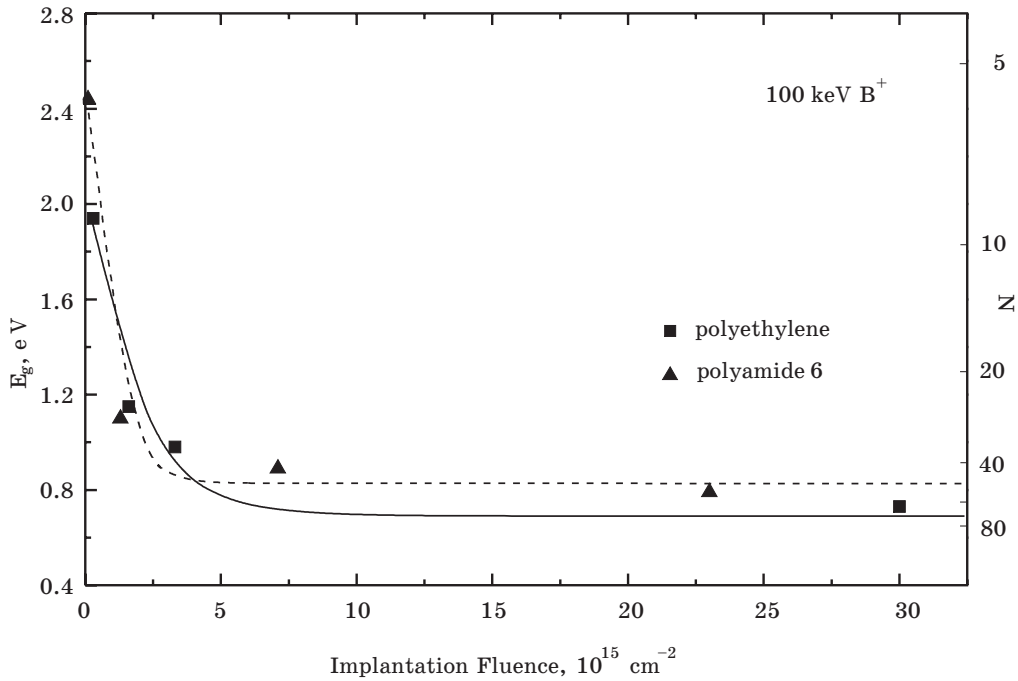

Fig. 4. Optical energy gap versus fluence for ion-implanted polyethylene and polyamide 6

$N \approx 60$). For polyamide 6, the formation of smaller carbon clusters is the result of the incorporation of heterocyclic nitrogen atom into the growing cluster. The outermost heteroatoms cannot play the role of nucleation sites of the carbon clusters and their presence in the clusters reduces the size of fragments of the π-electron conjugated system and, as a consequence, the effective size of carbon clysters determined from electronic spectra. It should be also noted that the obtained estimation of the cluster size is very rough since the Eq. (2) is valid for the case of compact clusters only (the decrease in the cluster compactness should result in more abrupt E_g *vs*. N dependence); moreover, it is well-known that Huckel theory overestimates the energies of the optical transitions in π-systems.

The optical spectroscopy thus enables to trace the major stages of carbonaceous phase formation in the course of the ion bombardment of a polymer: (i) formation of the initial carbon clusters and conjugated double bonds in the polymer host at doses below Φ_f, (ii) the growth of π-bonded clusters at higher doses, and (iii) completion of the cluster growth at high fluences. At the latter stage the most of the clusters reach their ultimate size which depends on the polymer nature and implantation conditions, with further implantation resulting only in rearrangements within the cluster aggregates.

The impact of the incoming ions on the polymer target and accompanying radiopyrolytic processes result in massive rupture of chemical bonds and lead to the formation of high concentrations of stable free radicals. Since these radicals are associated with carbon structures that appear under implantation, electron spin resonance (ESR) measurements can provide valuable information on the formation of a carbonaceous phase in the course of ion bombardment and on the transport properties of the ion-implanted polymers. The efficiency of the ESR spectroscopy in investigating of ion-induced transformations in the polymer host is also due to the fact that the most insulating polymers do not exhibit paramagnetic behavior prior to implantation.

The ESR spectra of ion-implanted polymers (polyethylene, polyimide, polyamide) consist of an isotropic singlet, with the lineshape being almost pure Lorenzian [4–6, 11, 14]. The narrow line width (1.5–2 G for high-fluenced samples – Fig. 5) and g values close to that of free electrons allow one to conclude that free radicals are delocalized in a π-system of carbon clusters. Studies of the fluence dependence of spin concentration show that a sharp rise in the spin concentration with the implanted dose is observed in the vicinity of Φ_f (Fig. 5). This can be attributed to the fact that the favorable conditions for the terminated carbon bonds compensation by interaction with atomic hydrogen exist at the initial stages of implantation. Moreover, the process of accumulation of the paramagnetic centers should strongly correlate with the formation of π-bonded carbon clusters, which ensure the stabilization of free radicals.

When in the course of carbonaceous phase formation the possibility of effective recombination of the terminated carbon bonds with each other appears, the intensity of the ESR signal exhibits saturation (Fig. 5). On the other hand, the linewidth narrowing with the implanted dose is observed, which is consistent with the increase in the electron spin exchange interactions. Taking into account the fact that the ESR linewidth and the conductivity of ion-irradiated polymer vary inversely (Fig. 5), one could conclude that delocalization of radicals is favored with a

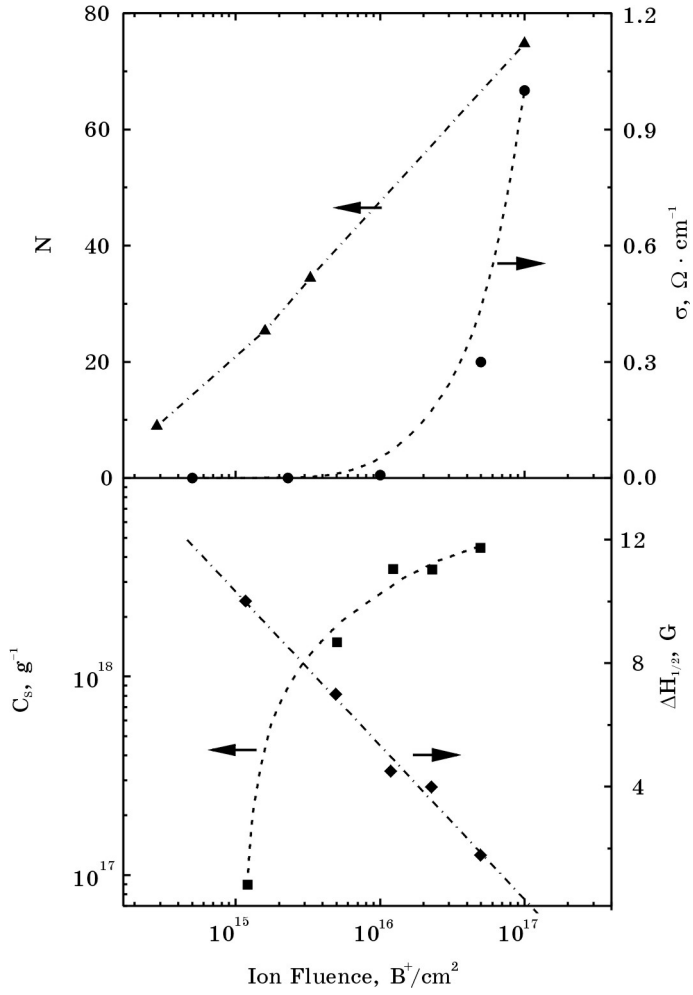

Fig. 5. The fluence dependence of the number of benzoid rings forming carbon cluster (N), d.c. conductivity (σ), spin concentration (C_s) and the linewidth ($\Delta H_{1/2}$) for polyethylene implanted with 100 keV B^+.

percolation cluster appearance. It should be also noted that since the linewidth is determined by the smallest π-bonded carbon clusters, the linewidth saturation value, which corresponds to the completion of the percolation cluster formation, is to be also dependent on the size distribution of carbon clusters in the implanted layer.

Studies of the temperature dependence of ESR lineshape in vacuum and under different oxygen pressures provide some further information on the charge transport properties of the ion-implanted polymers [2, 4, 5, 11, 15]. These studies have shown that the ESR linewidth for heavily implanted polymers does not depend on temperature in the range of 300–460 K (for instance, in the case of polyethylene

implanted with 100-keV B^+ ions the ESR linewidth cease to be temperature dependent at the doses above $2\times10^{16}cm^{-2}$, whereas in the case of polyimide implanted under the same conditions the linewidth turns out to be almost independent of the temperature over a wide fluence range). On the other hand, with highly-dosed polyethylene and polyimide the evacuation does not result in a decrease of the ESR signal amplitude. These facts evidence the formation of a quasi-two-dimensional degenerated electron gas in the conducting layer produced at the polymer surface under high-dose implantation.

ELECTRICAL AND ELECTROCHEMICAL PROPERTIES OF THE ION-IMPLANTED POLYMERS

In the case of normally insulating polymers, the conductivity increase resulting from the ion implantation is brought about not by chemical doping but by formation of π-bonded clusters in the implanted layer. As a result, the conductivity of the ion-implanted polymers does not depend directly on the nature of the implanted ions, being essentially determined by the energy losses of the incoming projectiles and on the energy deposition mechanism. On the other hand, since the conductive phase in the implanted layer is formed by discrete carbon clusters, the transition from insulating to the conducting state can be described as a percolative phase transition that leads to the following expression for conductivity σ:

$$\sigma \sim (x - x_c)^s, \tag{3}$$

where x the is relative concentration of the conductive clusters in the implanted layer, x_c is the critical concentration at which the percolation is possible, and s is the critical exponent. The existence of the threshold fluence, Φ_c, (corresponding to the current onset) is evident from the conductivity versus dose dependence (Fig. 5). In general, the following power law dependence of the percolation probability on the implanted dose holds:

$$x - x_c = (\Phi - \Phi_c)^y$$

and Eq.(3) can be thus rewritten as

$$\sigma \sim (\Phi - \Phi_c)^{ys} = (\Phi - \Phi_c)^t.$$

The values of t (the critical exponent for electrical conductivity versus fluence), obtained from the slope of $\log(\sigma)$ *vs.* $\log(\Phi - \Phi_c)$ linear dependencies for ion-irradiated polymers having aromatic or polyaromatic groups in their backbone (*e.g.*, polyimide), are 4–5 when the energy is deposited predominantly by the collissional mechanism, and 7–8 when the electronic stopping prevails. These values of the critical exponent for conductivity are substantially higher than those observed for metal nanoparticles in a dielectric matrix, which can be apparently explained by the effects of the conducting phase ordering during the implantation. On the other hand, for poorly carbonized polyethylene irradiated with 100-keV B^+ ions

the percolation threshold corresponds to $\Phi_c = 1.5 \times 10^{15}$ cm^{-2} (in this case, $\Phi_c > \Phi_f$) and the exponent t does not exceed a value of 2 that points to almost statistical formation of carbon clusters in the polymer host upon ion bombardment.

In the fluence range that corresponds to the appearance and growth of the fractal percolation cluster in the implanted layer, the temperature dependence of conductivity follows [4, 5]

$$\sigma \quad \sigma_0 \exp \quad T^*/T^{\ m} \ ,$$

where σ_o is the conductivity at the infinite temperature, m is the exponent for σ *vs.* T dependence which was found to be dependent on the implantation fluence (Fig. 6). The characteristic temperature T^* decrease rapidly with the implanted dose and the ion energy. When the carbon cluster formation occurs effectively, *i.e.* the implanted layer can be considered as a system of conductive grains in the dielectric matrix, the observed conductivity versus temperature dependence is consistent with charge transfer due to hopping between conductive islands ($m = 1/2$).

This model predicts the following dependence of the characteristic temperature on the morphology of the conducting layer: $T^* \propto (l/d)^2$ (where d is the effective diameter of the conductive island, l is the mean distance between the islands); a decrease in T^* with fluence may be thus explained by diminution of the mean hopping range when the concentration of the carbon clusters increases. Correspondingly, the rise in the cluster's size with the energy of the implanted ions implies a decrease in T^*. At high implantation doses, the transition from one-dimensional conductivity ($\log(\sigma)$ *vs.* $T^{-1/2}$) to three-dimensional one ($\log(\sigma)$ *vs.* $T^{-1/4}$) is observed for polyethylene and polyimide (Fig. 6). Furthermore, the possibility of the conjugated bonds formation between the carbon clusters at extra high fluences (>10^{17} cm^{-2}) can also affecting the dynamics of the charge transfer in the implanted layer and the exponent for temperature dependence of conductivity increases amounting $m \approx 3/4$. So, different variants of the ion-produced hopping conductivity can be observed in the case of normally insulating polymers upon ion implantation, the transport mechanism being dependent on the nature of the polymer and the implantation conditions. The situation is very similar to that observed in the case of traditional conducting polymers with conjugated bonds for which different charge transport mechanisms were also evident.

The electrochemical behavior of ion-implanted polymers is considerably affected by high sheet resistivity of the thin conducting layer formed under ion irradiation, because the potential drop in the implanted layer results in an increase of overvoltage when going from an electric contact along the electrode. As a consequence, only heavily dosed polymers have pronounced electrochemical activity (Fig. 7), and the polarization behavior of ion-implanted films is not consistent with Tafel law. In general, the current-voltage dependence for such a nonequipotential electrode may be described as follows

$$i \quad \sqrt{\frac{2hi_0RT}{\rho\alpha nF}\exp\frac{\alpha nF\eta}{RT}} \ ,$$

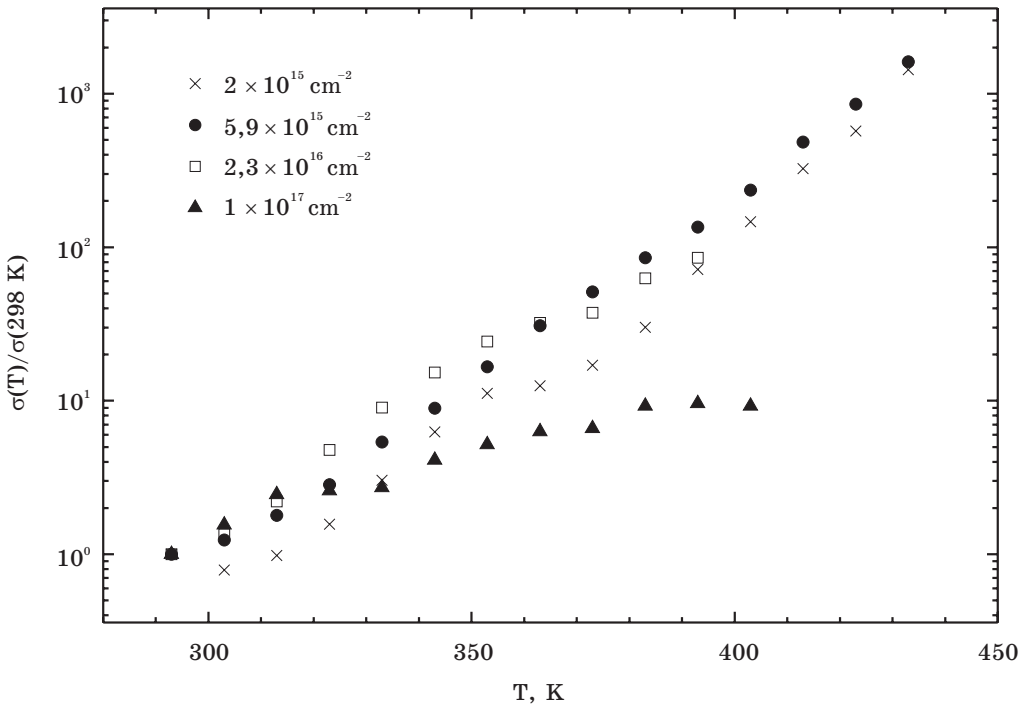

Fig. 6. Temperature dependence of d.c. conductivity for polyethylene implanted with 100 keV B^+ to different doses

where i is the current density, h and ρ are, respectively, the thickness and the specific resistivity of the implanted layer, i_0 is the exchange current density, α is the transfer coefficient, n is the number of electrons involved in the electrochemical reaction, and η is the overvoltage; other symbols have their traditional meanings. Ion-implanted polymer films with a buried carbonaceous layer can also function as electrodes owing to the high porosity of the implanted layer [4]. Because of the high exchange currents typical of carbon electrode materials, the electrodes based on the ion-implanted polymers generally operate in an unusual 'mixed' regime (at one end of the electrode the electrochemical reaction is governed by the interfacial kinetics, while at the other end the electrode reaction appears to be mainly under the diffusion control).

With anodic polarization and in contact with an indifferent electrolyte, ion-implanted polymers readily lose electrochemical activity due to oxidation of the carbonaceous conducting phase. With carbon electrode materials, the anodic reactions proceed *via* the formation of adsorbed hydroxyl radicals followed by their electrochemical desorption, which can be accompanied by the liberation of either CO_2 (destructive pathway) or oxygen (non-destructive pathway). Due to diffusion limitations in the surface nanopores, the slow degradation of the conducting carbonaceous phase, resulting in the electrode deactivation, also occurs when oxidation of the redox species proceeds at the surface of ion-implanted polymers. The

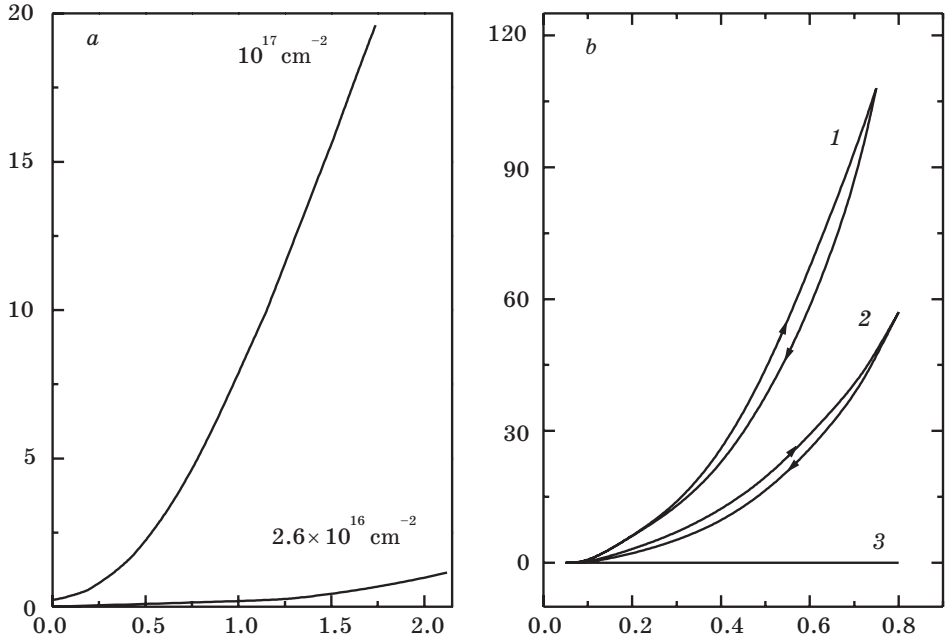

Fig. 7. Polarization curves for oxidation of (*a*) 10^{-1} M hydroquinone at polyamide 6 implanted with 100-keV B^+ to different doses; (*b*) 2×10^{-2} M ortho-phenylenediamine at polyethylene implanted with 100-keV B^+ to a dose 10^{17} cm^{-2}: the first cycle (curve *1*), the second cycle (curve *2*), the tenth cycle (curve *3*). Supporting electrolyte is 0.25 M Na_2SO_4.

destruction of carbonaceous nanophase is only slightly pronounced in the case of heavily fluenced polyimide and does not occur in the non-aqueous electrolytes. On the other hand, the electrochemical oxidation of *ortho*-phenylenediamine at the surface of ion-implanted polymer, that results in a growth of dielectric polymer interior the surface pores, permits one to seal hermetically the buried conductive layer (Fig. 7).

The distinctive features of ion-implanted polymers as the electrode material are (i) the buried conductive carbonaceous layer contacting with the electrolyte through the nanopores in the insulating surface layer and (ii) the variable sp^2/sp^3 ratio that opens the possibility of controlling the electrocatalytic properties of polymer electrode. In a broad sense, ion-implanted polymer films are intermediate in their electrocatalytic activity between glassy carbon and DLC.

The possibility of changing the surface conductivity of polymers in a very wide range by ion irradiation and the semiconductor-like behavior of ion-implanted polymers are of obvious interest for electronic device applications. Thus, the diodes and transistors can be produced by use of traditional approach to fabrication of semiconductor devices, as the ion implantation was employed to provide chemical or 'damage' doping of the organic semiconductors (*e.g.*, polyacetylene, PPV). On the other hand, it has already been mentioned that under some implantation conditions a buried carbon-rich layer can be formed within a dielectric poly-

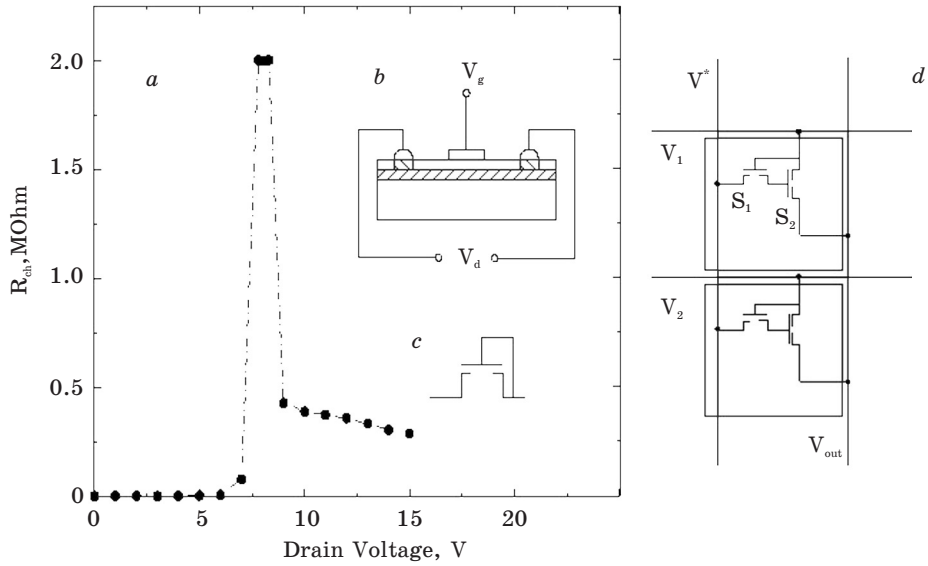

Fig. 8. (*a*) Resistance of the channel (R_{ch}) versus drain voltage (V_D) for the electronic switch based on ion-implanted polyethylene (resistance is measured at the frequency of 10 kHz); (*b*) a schematics of switch: the shaded region corresponds to the conducting channel produced in the polyethylene host by implantation of 100-keV B^+, the bonding pads for drain and source electrodes are made by implantation of 100-keV Sb^+, the gate was modified by electrochemical deposition of poly-*o*-phenylenediamine;(*c*) the measuring circuit; (*d*) the «neural» circuit taking a sum over all voltages $V_1 ... V_n$ higher than V^*, S_1 and S_2 are the switching devices havin the off threshold higher than V^*.

mer, the carbonaceous phase being separated from the surface of the sample by a nonconducting layer of a few tens of nm thick. This layer can be made more uniform by electrochemical deposition of nonconductive poly-*o*-phenylenediamine in the surface pores. The spatial characteristics of the obtained structure makes it possible to control the transconductance of the buried layer by applying an external electric field that opens the way for fabrication of transistor-like electronic switch [2, 4, 17]. An example of such electronic device is the polymer 'transistor' (Fig. 8) which operates in the a.c. mode at frequencies $> 10^3$ Hz, *i.e.*, under conditions where the hopping length diminishes to such extent that only the smallest clusters contribute to the conductivity. This device has a conducting channel formed by implantation of polyethylene with 100-keV B^+ ions up to a dose of 10^{17} cm^{-2}. The source and gate electrodes contacting with a buried channel were formed by a selective irradiation of the boron-implanted polymer sample with heavy ions providing the deep carbonization of the insulating surface layer, whereas the gate electrode was applied immediately on the boron-implanted surface modified with poly-*o*-phenylenediamine. It is seen from Fig. 8 that at some drain voltage the resistance of the channel rises abruptly, partial recovery of the channel conductance being observed at higher biases. It should be noted that, as in the case of a field-effect transistor with a channel made of ultrafine metal particles, the trans-

conductance of the buried channel produced in the polymer host *via* ion implantation can be controlled by applying both positive and negative gate voltages.

CONCLUSIONS

The experimental results discussed above indicate that ion beam-induced chemical processes in the polymer target are so much peculiar that are to be considered within the individual division of chemistry of high energies. These processes represent a kind of pulse thermoradiolysis which occurs in subnanosecond time scale and sometimes under conditions of massive ('non-thermodynamic') breakage of chemical bonds by nuclear collisions. Despite the fact that the energy transferred from the incident ions to the polymer matrix is rather high, the carbonization of the polymer surface observed under ion bombardment cannot be reduced to simple 'graphitization' of the polymer within the track of the stopping ion.

Ion implantation of high-energy ions into the initially dielectric polymers (polyethylene, polyamide) is accompanied with a profound radiopyrolytic transformations of polymer matrix leading to its dehydration and the formation of conductive carbonaceous phase built of carbon clusters of nanometer size (*ca.* ~ 2.5 nm in case of polyethylene implanted with 100-keV B^+). It has been shown that the chemical modification of polymer target under ion bombardment occurs *via* the following successive steps: (i) formation of radiation defects; (ii) growth of carbon clusters; (iii) completion of cluster growth and formation of conjugated double bonds between clusters at high fluences ($> 5 \times 10^{16}$ B^+/cm^2) accompanied with the increase in π-conjugation and formation of quasi-two-dimensional degenerated electron gas in the implanted layer. The Rutherford backscattering and neutron depth profiling studies of the distribution of the implanted boron and trapped oxygen, which decorates the dangling bonds produced under ion bombardment, have evidenced that ion beam-induced polymer carbonization becomes localized at some depth below the surface of the ion-irradiated polymer. As the result, the conductive carbon-rich layer produced upon ion implantation turns out to be separated from the surface of polymer target by highly-porous nonconducting layer 5–10 nanometers thick, and the continuity of the implanted layer may be enhanced by electrochemical deposition of insulating polymer in the surface pores. This opens the way for fabrication of polymer heterostructures with buried conductive layer, the transconductance of which can be effectively controlled by applying an external electric field, and developing of some radically new microelectronic, optoelectronic and electroanalytic polymer-based devices with the unusual characteristics.

ACKNOWLEDGEMENTS

This work was carried out in a close collaboration with the research group of Prof. V. Odzhaev (Department Physics, BSU). The author gratefully acknowledge the excellent assistance of the members of this group Dr. V. Popok, Dr. I. Azarko, Dr. I. Karpovich with the experiments recorded here.

REFERENCES

1. *Sviridov D.V.* // Russian Chemical Reviews. 2002.Vol. 74, № 4. P. 315-328.
2. *Sviridov D.V., Odzhaev V.B., Kozlov I.P.* Ion-Implanted Polymers. In: Electrical and Optical Polymer Systems /Ed. T. Wise. New York: Marcel Dekker Publ., 1998. P. 387–422.
3. *Odzhaev V. B., Kozlov I. P., Popok V. N., Sviridov D. V.* Ion implantation of polymers. Minsk: BSU. 1998. 197 p.
4. *Azarko I. I., Karpovich I. A., Kozlov I. P., Odzhaev V. B., Sviridov D. V.* // Poverhnost. 1999. № 11. P. 80–84.
5. *Odzhaev V.B., Azarko I.I., Karpovich I.A., Kozlov I.P., Popok V.N., Sviridov D.V., et al.* // Materials Letters. 1995. Vol. 23, № 2. P. 163–166.
6. *Popok V. N., Odzhaev V. B., Kozlov I. P., Azarko I. I, Karpovich I. A., Sviridov D. V.* // Nucl. Instr. and Meth. B. 1997. Vol. 129. P. 60–64.
7. *Kozlov I. P., Odzhaev V. B., Karpovich I. A., Popok V. N., Sviridov D. V.* // J. Appl. Spectoscopy. 1998. Vol. 65, № 3. P. 390–394.
8. *Popok V., Sviridov D.* // Atomic Collisions in Solids: Abstr. of the 18th Int. Conf. Odense, 1999. P. 110.
9. *Popok V. N., Karpovich I. A., Odzhaev V. B., Sviridov D. V.* // Nucl. Instr. and Meth. B. 1999. Vol.148. P. 1106–1110.
10. *Azarko I. I., Karpovich I. A., Kozlov I. P., Krasovski S. V., Odzhaev V. B., Popok V. N., Sviridov D. V., Sergeev S. P.* // Proc. Int. Conf. "The Current State and Prospects of Scientific Researches in the Byelorussian State Polytechnic Academy". Minsk, 1995. P. 64–65.
11. *Azarko I. I., Karpovich I. A., Kozlov I. P., Odzhaev V. B., Popok V. N., Sviridov D. V.* // Polymer Mater. Sci. Eng.: Proc of the 209th ACS Nat. Meeting. Anaheim (USA), 1995. P. 337.
12. *Odzhaev V. B., Popok V. N., Azarko I. I., Karpovich I. A., Kozlov I. P., Sviridov D. V., Krasovskij S. V.* // Proc. of the 10th Int. Conf. on Ion Beam Modification of Materials. Albuquerque (USA), 1996. N39.
13. *Popok V., Karpovich I., Odzhaev V., Sviridov D.* // Proc. of the 11th Int. Conf. on Ion Beam Modification of Material. Amsterdam (Netherlands), 1998. P. 21–22.
14. *Kozlov I., Odzhaev V., Popok V., Azarko I., Karpovich I., Sviridov D.* // Proc. of the 5th Symp. Nauk.-Technicz. «Technologie Electrostatyczne i Electonowo-Ionowe». Augustov (Poland), 1997. P. 88–94.
15. *Kozlov I. P., Odzhaev V. B., Popok V. N., Azarko I. I., Sviridov D. V.* // The 2nd Int. Conf. "Interaction of Radiations with Solids". Minsk, 1997. P. 119.
16. *Azarko I., Karpovich I., Kozlov I., Odzhaev V., Popok V., Sviridov D., Jankovskij O.* // Proc. of Int. Symp. «Ion Implantation of Science and Technology». Naleczow (Poland), 1997. P. 80–83.
17. *Karpovich I. A., Kozlov I. P., Odzhaev V. B., Azarko I. I., Sviridov D. V.* Pat. C1 BY (H 01L 29/51). № 2259 (Belarus). Appl. 28.11.94, Reg. 03.03.1998.
18. *Azarko I. I., Karpovich I. A., Kozlov I. P., Odzhaev V. B., Popok V. N., Sviridov D. V.* // Proc. of Conf. "Actual Problems of Social and Natural Sciences". Minsk, 1996. P. 158–160.
19. *Popok V., Odzhaev V., Azarko I., Sviridov D., Hnatowicz V., Vacik J., Cervena J.* // Proc. of 10th Int. Conf. on Radiation Effects in Insulators. Jena, 1999. P. 245.
20. *Popok V. N., Odzhaev V. B., Azarko I. I., Kozlov I. P., Sviridov D. V.* // Nucl. Instrum. Methods B. 2000. Vol. 166–167. P. 660–663.